Simulations of Hierarchical Basis Reachability Graphs

Ziyue Ma, Guanghui Zhu, Zhiwu Li

February 16, 2020

In this note we report two benchmarks of *Hierarchical Basis Reachability Graphs* (HBRGs). Results are carried out on a laptop computer with Intel i5-4200M 2.5 GHz processor and 8 GB DDR3 1600Hz RAM.

1 Benchmark 1

The net in Figure 1 is slightly modified from Figure 5 in [1], a Petri net modeling a complex automatic manufacturing system. Comparing with the net in [1], two self-looped arcs ($t_{33} \leftrightarrow p_6$, $t_{36} \leftrightarrow p_{21}$) and one directed arcs ($t_{39} \rightarrow p_{46}$) are removed. This net contains 46 places and 39 transitions. The set of observable transitions contains 24 transitions:

$$T_o = \{t_1, t_3, t_6, t_7, t_8, t_9, t_{13}, t_{14}, t_{15}, t_{16}, t_{20}, t_{21}, t_{22}, t_{23}, t_{24}, t_{26}, t_{28}, t_{29}, t_{30}, t_{31}, t_{32}, t_{34}, t_{35}, t_{39}\}.$$

The initial marking shown in the figure is parameterized as: $M_0 = a \cdot p_1 + b \cdot p_{16} + p_{31} + p_{32} + p_{33} + p_{34} + p_{35} + p_{37} + p_{38} + p_{39} + 8p_{40} + p_{41}$.

1.1 Hierarchical Partition I

Consider a hierarchical partition $T_o = T_{pri} \cup T_{sec}$ where the primary observable transitions (11 in total, marked in blue in Figure 1) are:

$$T_{pri} = \{t_1, t_3, t_7, t_9, t_{14}, t_{20}, t_{22}, t_{24}, t_{29}, t_{32}, t_{35}\}$$

and the secondary observable transitions (13 in total, marked in red in Figure 1) are:

$$T_{sec} = \{t_6, t_8, t_{13}, t_{15}, t_{16}, t_{21}, t_{23}, t_{26}, t_{28}, t_{30}, t_{31}, t_{34}, t_{39}\}.$$

The simulation results for computing BRGs (with respect to $T_E = T_o$) and HBRGs are summarized in Table 1. One can see that when the initial marking is not so small (entries 3 to 8), the size of an HBRG is less than 15% of that of the RG: such a ratio is continuously decreasing when the size of RG increases. Although the size of an HBRG is about twice as large as that of the corresponding BRG, the time consumption to compute an HBRG is only about 5% of that to compute the BRG.

a	b	RG	BRG	τ_B	HBRG	τ_H	HBRG/RG	τ_H/τ_B
1	1	1966	680	0.095	849	0.069	43.1%	72.6%
1	2	12577	3180	0.574	4447	0.352	35.3%	61.3%
1	3	44942	8828	2.017	13051	0.696	29.0%	34.5%
2	2	76808	13214	4.165	19469	0.572	25.3%	13.7%
2	3	262236	35498	46.126	53695	1.446	20.4%	3.1%
2	4	586604	68114	191.147	103504	3.428	17.6%	1.8%
3	3	853850	87038	296.763	133286	4.536	15.6%	1.5%
3	4	1837329	163470	1148.951	248119	11.739	13.5%	1.0%

Table 1: Simulations results of Benchmark 1.1 with different values of a and b. RG, BRG, and HBRG denote the numbers of markings/nodes in the reachability graph, BRG, and HBRG, respectively. τ_B and τ_H are time-consumptions (in *seconds*) to compute BRG and HBRG, respectively.

1.2 Hierarchical Partition II

Consider the same net but a different hierarchical partition $T_o = T_{pri} \cup T_{sec}$ where the primary observable transitions are:

$$T_{pri} = \{t_3, t_6, t_8, t_9, t_{13}, t_{15}, t_{16}, t_{20}, t_{22}, t_{24}, t_{28}, t_{29}, t_{31}, t_{34}\}$$

and the secondary observable transitions are:

$$T_{sec} = \{t_1, t_7, t_{14}, t_{21}, t_{23}, t_{26}, t_{30}, t_{32}, t_{35}, t_{39}\}.$$

Transitions in sets T_{pri} and T_{sec} are marked in blue and red, respectively, in Figure 2. The simulation results for computing BRGs (with respect to $T_E = T_o$) and HBRGs are summarized in Table 2.

a	b	RG	BRG	τ_B	HBRG	τ_H	HBRG/RG	τ_H/τ_B
1	1	1966	680	0.124	720	0.098	36.6%	79.0%
1	2	12577	3180	0.467	3720	0.117	29.5%	25.1%
1	3	44942	8828	1.909	10924	0.365	24.3%	19.1%
2	2	76808	13214	4.202	16914	0.643	22.0%	15.3%
2	3	262236	35498	46.289	48184	2.425	18.3%	5.2%
2	4	586604	68114	196.664	95714	8.705	16.3%	4.4%
3	3	853850	87038	293.817	122576	10.716	14.3%	3.6%
3	4	1837329	163470	1171.856	238450	39.892	12.9%	3.4%

Table 2: Simulations results of Benchmark 1.2 with different values of a and b. RG, BRG, and HBRG denote the numbers of markings/nodes in the reachability graph, BRG, and HBRG, respectively. τ_B and τ_H are time-consumptions (in *seconds*) to compute BRG and HBRG, respectively.

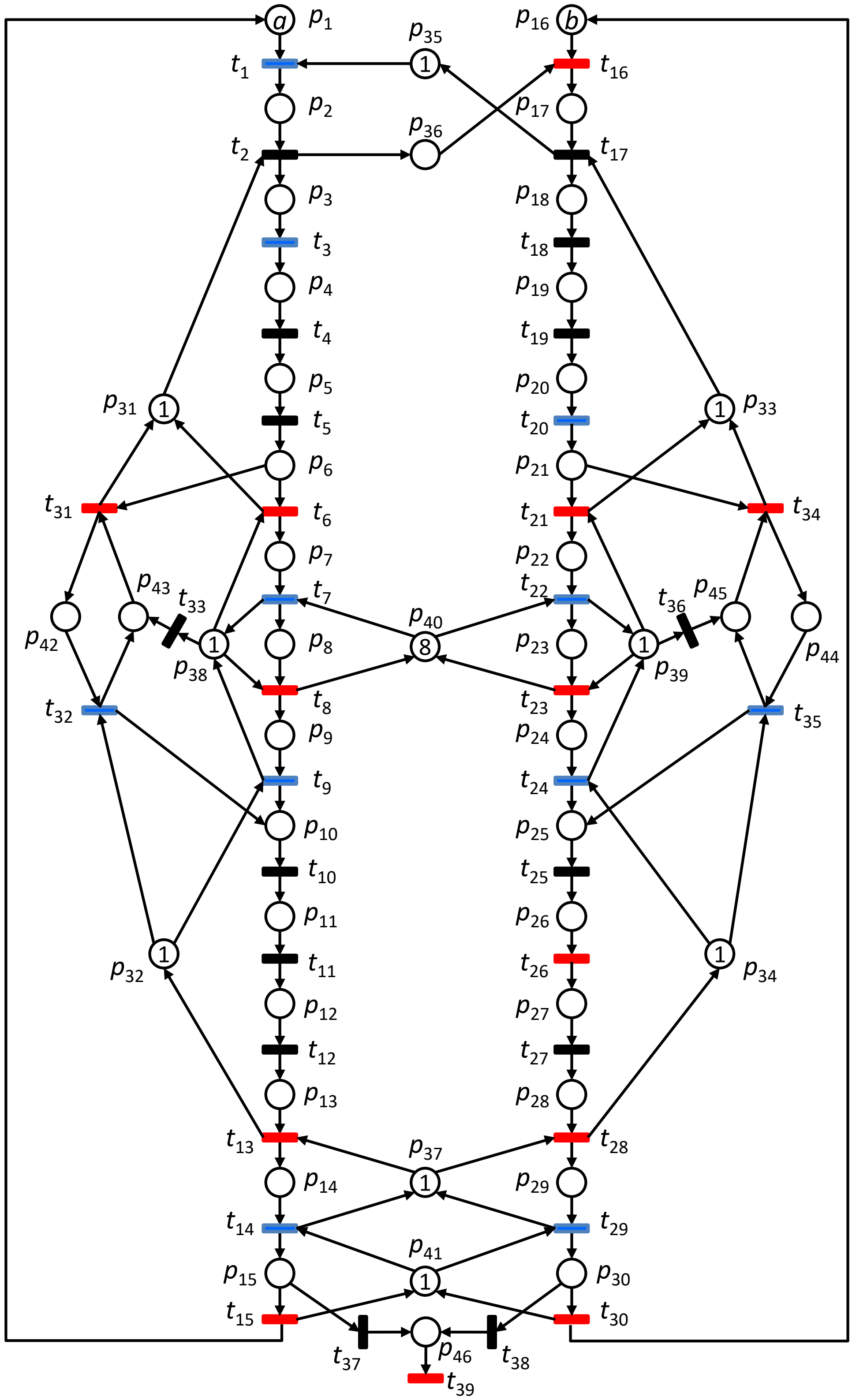

Figure 1: Benchmark 1.1. Sets $T_{pri} = \{t_1, t_3, t_7, t_9, t_{14}, t_{20}, t_{22}, t_{24}, t_{29}, t_{32}, t_{35}\}$ (blue), $T_{sec} = \{t_6, t_8, t_{13}, t_{15}, t_{16}, t_{21}, t_{23}, t_{26}, t_{28}, t_{30}, t_{31}, t_{34}, t_{39}\}$ (red).

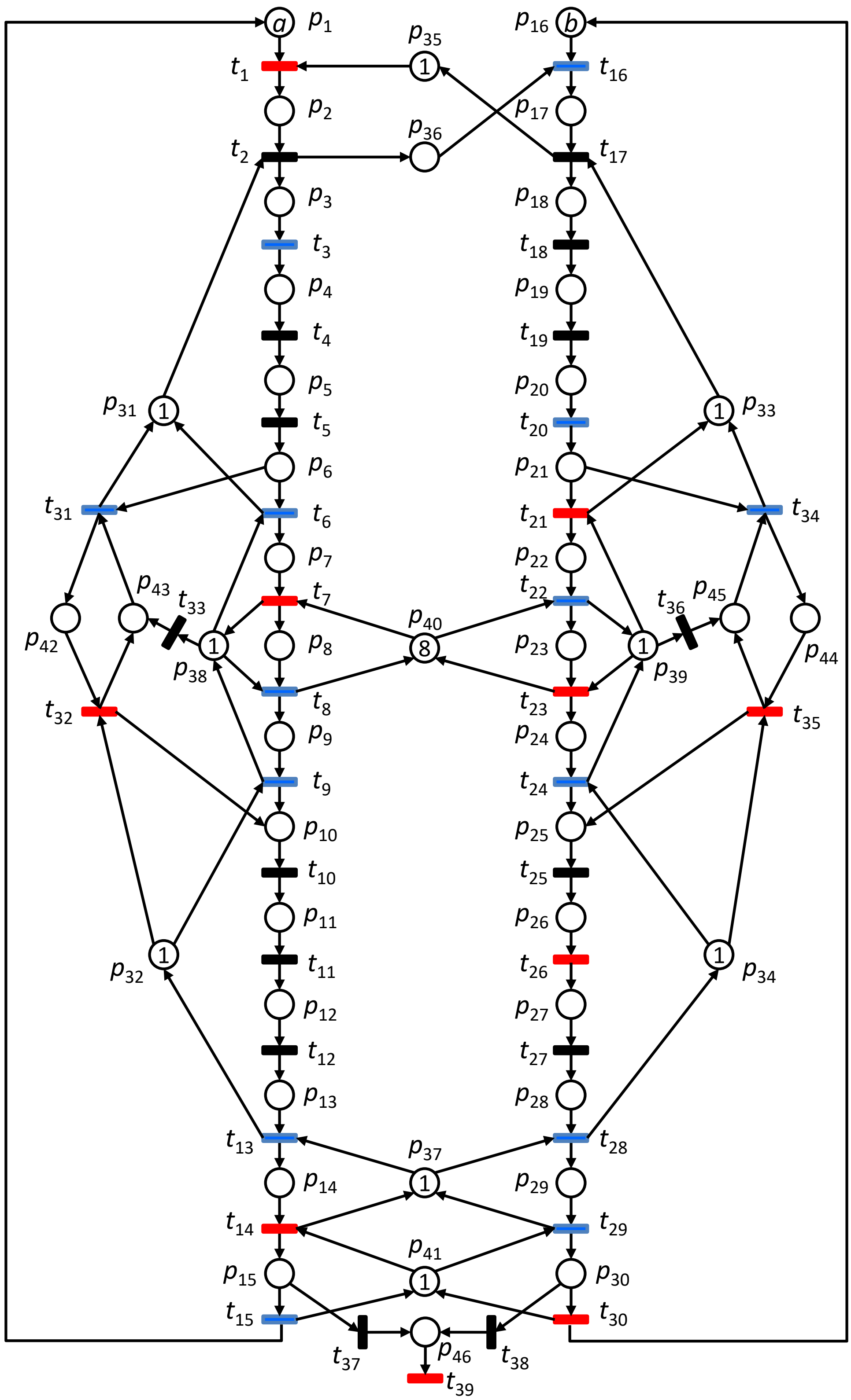

Figure 2: Benchmark 1.2. Sets $T_{pri} = \{t_3, t_6, t_8, t_9, t_{13}, t_{15}, t_{16}, t_{20}, t_{22}, t_{24}, t_{28}, t_{29}, t_{31}, t_{34}\}$ (blue), $T_{sec} = \{t_1, t_7, t_{14}, t_{21}, t_{23}, t_{26}, t_{30}, t_{32}, t_{35}, t_{39}\}$ (red).

2 Benchmark 2

The net in Figure 3 is taken from [2] which models a series of parallel work-flows. This net has three parameters: the number of work-flows (as well as the weight from p_1 to t_1) n, the length of each work-flows m, and the initial number of tokens $M_0(p_1) = a$. The set $T_o = T_{pri} \cup T_{sec}$, where the set T_{pri} (marked in blue) is parameterized as:

$$T_{pri} = \{t'_{km+1} \mid k = 1, \ldots, n\} \cup \{t''_{km+1} \mid k = 1, \ldots, n\}$$

and the set T_{sec} (marked in red) is parameterized as:

$$T_{sec} = \{t'_{k1} \mid k = 1, \ldots, n-1\} \cup \{t'_{km} \mid k = 2, \ldots, n\} \cup \{t''_{km} \mid k = 2, \ldots, n\}.$$

The simulation results of the BRGs (with respect to $T_E = T_o$) and HBRGs for different (n, m, a)'s are summarized in Table 3. In this simulation, the size of HBRG is slightly larger than the size of a BRG, but the time consumption to compute an HBRG is much smaller, especially in the case where the size of RG and BRG is large (the last two entries).

n	m	a	RG	BRG	τ_B	HBRG	τ_H	HBRG/RG	τ_H/τ_B
2	1	4	121	81	0.009	81	0.002	66.9%	22.2%
2	2	4	361	108	0.013	81	0.003	22.4%	23.1%
2	3	4	841	108	0.019	81	0.007	9.6%	36.8%
2	1	6	1648	1323	0.064	1323	0.022	80.2%	34.6%
2	2	6	9460	2106	0.256	1323	0.020	13.9%	7.8%
2	3	6	36205	2106	0.258	1323	0.027	3.6%	10.5%
3	1	6	2025	486	0.046	486	0.015	24.0%	32.6%
3	2	6	10000	648	0.108	648	0.022	6.4%	20.4%
3	3	6	34225	648	0.124	648	0.039	1.8%	31.5%
3	1	9	126905	40095	62.181	40095	0.603	31.6%	1.0%
3	2	9	1764787	65232	219.673	65232	1.556	3.7%	0.7%
3	3	9	13168689	65232	211.705	65232	1.443	0.5%	0.7%

Table 3: Simulations results of Benchmark 2 with different values of n, m, a.

References

[1] M. Cabasino, A. Giua, M. Pocci, and C. Seatzu, “Discrete event diagnosis using labeled Petri nets: an application to manufacturing systems,” *Control Engineering Practice*, vol. 19, no. 9, pp. 989–1001, 2011.

[2] M. P. Cabasino, A. Giua, L. Marcias, and C. Seatzu, “A comparison among tools for the diagnosability of discrete event systems,” in *Proceedings of the 2012 IEEE International Conference on Automation Science and Engineering*, Aug 2012, pp. 218–223.

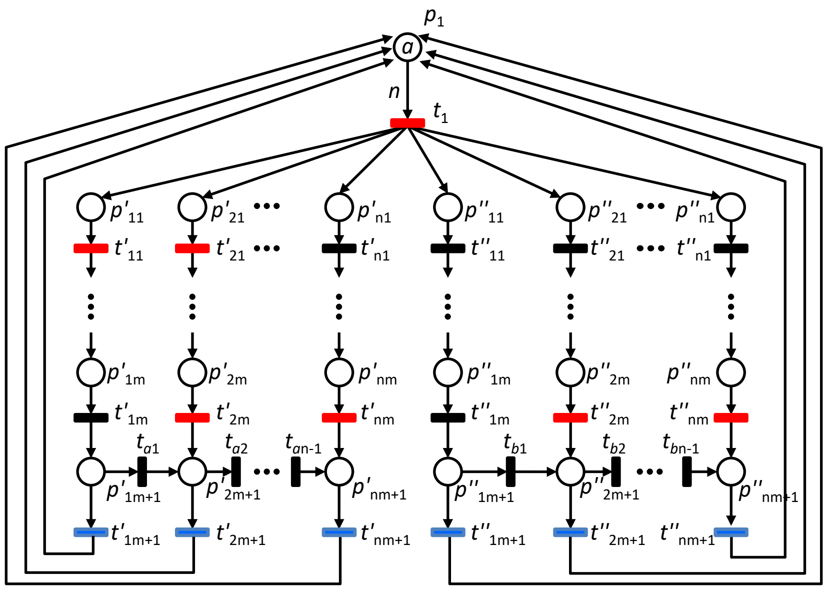

Figure 3: Benchmark 2. Transitions in sets T_{pri} and T_{sec} are marked in blue and red, respectively.